宮崎大学学術情報リポジトリ
University of Miyazaki Academic Repository

Protective role of estrogen through G-protein coupled receptor 30 in a colitis mouse model

メタデータ	言語: English 出版者: Springer Science and Business Media LLC 公開日: 2024-10-10 キーワード (Ja): キーワード (En): CDX2, Colitis, Estrogen, GPR30, Histone modification 作成者: Fidya, チヨウジヨウフ, ナランツオツク, 池ノ上, 実, 矢野, 公一, 山隈, 優, 白水, 慎一郎, 甲斐, 健吾, 石塚, 匠, 菱川, 善隆 メールアドレス: 所属:
URL	http://hdl.handle.net/10458/0002000804

This version of the article has been accepted for publication, after peer review (when applicable) and is subject to Springer Nature’s AM terms of use, but is not the Version of Record and does not reflect post-acceptance improvements, or any corrections. The Version of Record is available online at: http://dx.doi.org/10.1007/s00418-023-02235-z

Protective role of estrogen through G-protein coupled receptor 30 in a colitis mouse model

Fidya[1,2], Narantsog Choijookhuu[1], Makoto Ikenoue[1,3], Koichi Yano[1,3], Yu Yamaguma[1,4], Shinichiro Shirouzu[1,4], Kengo Kai[1,3], Takumi Ishizuka[1] and Yoshitaka Hishikawa[1]

[1]Department of Anatomy, Histochemistry and Cell Biology, Faculty of Medicine, University of Miyazaki, 5200 Kihara, Kiyotake, Miyazaki 889-1692, Japan

[2]Department of Oral Biology, Faculty of Dentistry, Universitas Brawijaya, Malang, Jawa Timur, Indonesia

[3]Department of Surgery, Faculty of Medicine, University of Miyazaki, 5200 Kihara, Kiyotake, Miyazaki 889–1692, Japan

[4]Department of Oral and Maxillofacial Surgery, Faculty of Medicine, University of Miyazaki, 5200 Kihara, Kiyotake, Miyazaki 889-1692, Japan

Correspondence:

Yoshitaka Hishikawa, MD., Ph.D.,

Department of Anatomy, Histochemistry and Cell Biology, Faculty of Medicine, University of Miyazaki, 5200 Kihara, Kiyotake, Miyazaki 889-1692, Japan. Tel: +81-985-85-1783. Fax: +81-985-85-9851 E-mail: yhishi@med.miyazaki-u.ac.jp

Running title: Protective role of GPR30 in mouse colitis.

Abstract

Estrogen and its receptors are involved in the pathogenesis of gastrointestinal diseases such as colitis. However, the role of the membrane estrogen receptor G-protein–coupled receptor 30 (GPR30) in colitis is poorly understood. We therefore investigated the effect of estrogen in dextran sulfate sodium (DSS)-induced colitis. Male C57BL/6 mice were administered 1.5% DSS for 5 days and treated with 17β-estradiol (E_2), GPR30 agonist (G1), or GPR30 antagonist (G15) for 8 days. Inflammation grade was evaluated by disease activity index (DAI) and histomorphological score. Colon tissues were immunohistochemically analyzed and revealed high expression of membrane GPR30, histone 3 lysine 36 dimethylation, and lysine 79 trimethylation in normal mouse colon epithelial cells but significantly decreased expression in DSS-treated mice, whereas the expression was partially preserved after treatment with E_2 or G1. Colon shortening and DAI were significantly lower in E_2- and G1-treated mice compared to DSS-treated mice. Caudal type homeobox 2 (CDX2) expression and cell proliferation differed in normal colon epithelial cells but overlapped in those of DSS-treated mice. Administration of E_2 and G1 reduced CDX2 expression and cell proliferation. Altered expression of claudin-2 and occludin were observed in the colonic epithelium of DSS-treated mice, and these changes were significantly lower in the colon of E_2- and G1-treated mice. These results indicate that estrogen regulates histone modification, cell proliferation, and CDX2 expression through GPR30, which affects intestinal epithelial barrier function. We conclude that estrogen protects against intestinal epithelial damage through GPR30 by enhancing intestinal epithelial barrier function in DSS-induced colitis in mice.

Keywords: Estrogen**,** GPR30, colitis, histone modification, CDX2

Introduction

Inflammatory bowel disease (IBD) is an inflammation of the gastrointestinal tract caused by imbalances in several factors, including the environment, intestinal microbes, and epigenetic modifications (Ali et al. 2018; Dalal and Chang 2014). Numerous studies have investigated the pathways affected by inflammation as a target of potential epigenetic changes and their relationship to IBD pathogenesis (Mateos et al. 2019). Therefore, treating IBD via epigenetic regulation may be a promising target therapy. The incidence of ulcerative colitis, a type of IBD, is reportedly increasing and is associated with a more severe clinical course in males than females (Forss et al. 2022; Shivashankar et al. 2017), suggesting that the sex hormone estrogen and its receptor may be involved (Bábíčková et al. 2015; Goodman et al. 2018; Verdú et al. 2002). The membrane estrogen receptor G-protein–coupled receptor 30 (GPR30) is expressed in the gastrointestinal tract and plays an important role in the physiology and pathophysiology of the colon, including conditions such as IBD (Jacenik et al. 2019; Zielińska et al. 2017). However, the functional role of GPR30 and its relationship to epigenetic regulation in colitis remain poorly understood.

The pathogenesis of colitis begins with a leaky gut, which allows bacterial-derived compounds to enter the mucosa and trigger inflammation through the phosphatidylinositol-3-kinase (PI3K) and mitogen-activated protein kinase/extracellular signal–regulated kinase (MAPK/ERK) signaling pathways (Chelakkot et al. 2018; Heller et al. 2008; Mankertz et al. 2009). Activation of these pathways results in increased expression of the transcription factor caudal type homeobox 2 (CDX2), which regulates intestinal barrier function (Kaimaktchiev et al. 2004; Suzuki et al. 2011). In addition, the expression of tight-junction proteins that maintain intestinal permeability is altered in ulcerative colitis compared to normal human colon (Tan et al. 2019). The change in CDX2 expression leads to the disruption of intestinal epithelial homeostasis (Luettig et al. 2015). Therefore, CDX2-targeted treatments could become promising novel therapies for IBD.

71 In this study, we investigated the protective role of estrogen by examining the function of
72 GPR30, its involvement in epigenetic regulation, and the effect on CDX2 and impact on intestinal
73 permeability in a dextran sulfate sodium (DSS) -induced colitis mouse model. First, we performed
74 immunohistochemistry analyses to determine the localization of GPR30, histone 3 lysine 36
75 dimethylation (H3K36me2), and histone 3 lysine 79 trimethylation (H3K79me3) in colon epithelial
76 cells of DSS-treated mice. Expression of CDX2 and its co-localization with a marker of
77 proliferating cells was examined using double immunofluorescence analysis. Finally, the
78 expression of claudin-2 and occludin was analyzed to examine the effect of estrogen treatment on
79 epithelial tight junction proteins.
80

Materials and methods

Chemicals and biochemicals

DSS (molecular weight 36,000-50,000) was purchased from MP Biomedicals (Solon, OH, USA); 17β-estradiol (E_2), bovine serum albumin (BSA), 3-aminopropyl-triethoxysilane, and Brij L23 were obtained from Sigma-Aldrich (St. Louis, MO, USA); and GPR30 agonist (G1) and GPR30 antagonist (G15) were obtained from Tocris Bioscience (Bristol, UK). Paraformaldehyde (PFA) was purchased from Merck (Darmstadt, Germany); 3,3′-diaminobenzidine–4 HCl (DAB) was purchased from Dojindo Chemicals (Kumamoto, Japan), and all other chemicals used in this study were obtained from Fujifilm Wako Pure Chemicals (Osaka, Japan).

Animals and tissue preparation

Male C57BL/6 mice (8 weeks old) were used in this study (Japan SLC Inc.) and kept under constant 12-h dark/light conditions and fed standard chow with drinking water *ad libitum* with a 1-week acclimation period. The experimental protocol was approved by the Animal Ethics Review Committee of the University of Miyazaki (2021-521-2). The experimental animals were divided into control, DSS, DSS+E_2, DSS+E_2+G15, DSS+G1, and DSS+G1+G15 groups; each group consisted of 3-5 mice. Drinking water containing 1.5% DSS was given for 5 consecutive days to induce acute colitis in the mice. On day 5, the DSS solution was replaced with drinking water and continued for 3 days. Control mice received normal drinking water.

E_2 powder was dissolved in 100% ethanol (EtOH) and administered with saline daily via intraperitoneal (i.p.) injection at 100 μg/kg body weight from 1 day before DSS was given until day 8. Control and DSS-treated mice received daily i.p. injections of EtOH in saline. G1 and G15 powder was dissolved in dimethyl sulfoxide (DMSO)/saline. G1 was delivered by i.p. injection at 1 mg/kg body weight, while the dose of G15 was approximately 7-fold excess to E_2 and G1, as

105 described in a previous study (De Francesco et al. 2014). The disease activity index (DAI) score,
106 consisting of scores for weight loss, stool consistency, and rectal bleeding, was evaluated every 2
107 days (Gonçalves et al. 2013). Mice were sacrificed on day 8, the colon was removed from the
108 cecum to the rectum, and then the length was measured. The colon was opened longitudinally, fixed
109 in 4% PFA in PBS overnight at room temperature, and embedded in paraffin.
110

111 **Histological analysis**

112 Paraffin-embedded colon tissue was sectioned on a microtome at 4-µm thickness. The
113 microscopic morphology of the tissue was analyzed by hematoxylin and eosin (HE) staining.
114 Histomorphologic scoring was determined using three parameters: pathological crypt changes,
115 extent of involvement in the hyperplastic epithelium, and infiltration of inflammatory cells (Cooper
116 et al. 1993).
117

118 **Immunohistochemistry analysis**

119 Tissue sections were deparaffinized with toluene and rehydrated with a graded ethanol
120 series before being autoclaved in 10 mM citrate buffer for 15 min at 120°C (pH 6.0) (Yamaguma
121 et al. 2022; Yano et al. 2022). Endogenous peroxidase activity was blocked by incubation with 3%
122 hydrogen peroxide (H_2O_2) in methanol for 15 min for the anti-GPR30 antibody and 0.3% H_2O_2 for
123 other antibodies then rinsed with PBS three times for 5 min each. To block non-specific binding of
124 antibodies, tissue sections were treated with 500 µg/ml of normal goat IgG and 1% BSA in PBS
125 for 1 h. After blocking, the sections were reacted overnight with the following primary antibodies:
126 GPR30 (Abcam, #ab39742), H3K36me2 (Cell Signaling, 2901), H3K79me3 (Cell Signaling,
127 4260), CDX2 (Abcam, #ab76541), PCNA (Dako, M0879), claudin-2 (Abcam, #ab39742), and
128 occludin (Abcam, #ab216327). The sections were then washed in 0.075% Brij/PBS and incubated

129 with horseradish peroxidase–labeled secondary antibodies (Dako, P0447, P0048) for 1 h. After
130 washing with 0.075% Brij/PBS, sections were visualized using DAB and H_2O_2 (brown). For
131 immunofluorescence analysis, sections were reacted with FITC-conjugated tyramide, Alexa-546–
132 conjugated goat anti-mouse IgG for PCNA, or Alexa-488–conjugated goat anti-rabbit IgG for
133 CDX2 and then counterstained with DAPI (Choijookhuu et al. 2022; Shirouzu et al. 2022). As a
134 negative control, a normal mouse and rabbit IgG were used at the same concentration instead of
135 the primary antibody in each experiment. Microphotographs were taken using an Olympus DP74
136 camera and Olympus BX53 light microscope (CellSens Imaging Software, version 3.1).
137 Fluorescent micrographs were taken using DAPI (excitation 360 nm), FITC (excitation 470 nm),
138 and TRITC (excitation 545 nm) filters with a Keyence BZ-X700 microscope.
139

140 **Quantitative analysis**

141 The ratio of membrane and nuclear expression of GPR30 was determined in 3 mice per
142 experimental group. In each mouse, 6 micrographs including the middle and distal colon areas were
143 used for quantitative analysis. Expression of GPR30, CDX2, claudin-2, and occludin (brown color
144 in DAB staining) was measured using ImageJ software, version 1.53 (NIH, USA), with *red* color
145 assigned to positive cells using WinROOF software, version 7.0 (Mitani, Tokyo, Japan). Five fields
146 were randomly selected for analysis for each sample. Nuclear expression was measured by
147 numbering each positive epithelial cell, and then the number of the marked area was calculated.
148 For cell membranes, positive staining was evaluated based on the staining density over the level of
149 staining in the control group.
150

151 **Statistical analysis**

152 All data are expressed as the mean ± standard error of the mean (SEM). The One-way
153 ANOVA test was used to determine statistical significance among the groups, set as $p<0.05$. We
154 continued with the Tukey HSD test to analyze differences between groups. The Statistical Package
155 for Social Sciences (SPSS version 20, Chicago, IL, USA) was used for all analyses.
156

157 **Results**

158 **Estrogen treatment decreased the severity of inflammation in DSS-induced colitis**

159 A schematic representation of DSS-induce colitis in mice is shown in Figure 1a. Colon
160 length was measured in all experimental groups to examine the gross morphological changes (Fig.
161 1b). The DSS group showed the shortest colon length (5.5 ± 0.1 cm). The E_2 and G1 administration
162 groups (DSS+E_2; DSS+G1) exhibited less shortening of the colon length (6.9 ± 0.2 cm and 7.0 ±
163 0.1 cm, respectively), but the antagonist G15 administration groups (DSS+E_2+G15;
164 DSS+G1+G15) exhibited shortened colon length similar to that of the DSS treatment group (Fig.
165 1c). The DAI score was higher in the DSS group (6.7 ± 0.2) compared to the control group. The E_2
166 and G1 treatment groups exhibited significantly lower DAI scores (3.1 ± 0.2 and 3.3 ± 0.1,
167 respectively) than the DSS and antagonist groups (Fig. 1d). Histomorphological scores were also
168 higher in the DSS (3.4 ± 0.1) and antagonist-treated groups compared with the control group. The
169 histomorphological score was lower in the DSS+E_2 (2.2 ± 0.1) and DSS+G1 treatment (1.95 ± 0.1)
170 groups compared to DSS group (Fig. 1e, f), which confirmed that E_2 and G1 protect against severe
171 damage in DSS-induced colitis.

172

173 **Subcellular localization of GPR30 in DSS-induced colitis**

174 Immunohistochemical analysis was used to determine the subcellular localization of
175 GPR30 in mouse colon epithelial cells. GPR30 expression was observed in the epithelial cell
176 membrane and nucleus (Fig. 2a). Immunohistochemistry analysis revealed two distinct expression
177 patterns of GPR30: predominantly in the cell membrane, and in the nucleus. In normal colon,
178 GPR30 expression was mainly found in the cell membrane. Quantification of the
179 immunohistochemistry results revealed that the membrane expression of GPR30 was reduced in
180 the DSS (3762 ± 587 pixels) and antagonist groups compared with the control group (33820 ± 1545

181 pixels) (Fig. 2b). Positive cell nucleus localization of GPR30 expression was found predominantly
182 in the DSS (122 ± 1) and antagonist groups, but the nuclear expression was lower in the control
183 (23 ± 1), DSS+E_2 (51 ± 2), and DSS+G1 (43 ± 1) groups (Fig. 2c).
184

185 **Alteration of histone methylation in DSS-induced colitis**

186 Our results indicated reduced H3K36me2 (Fig. 3a) and H3K79me3 (Fig. 3b) expression in
187 the DSS group compared with the control group. In contrast, expression of both proteins was
188 partially preserved in DSS mice treated with E_2 or G1. The antagonist group also exhibited reduced
189 H3K36me2 and H3K79me3 expression in epithelial cells. There were no significant differences in
190 the expression of other dimethylated or trimethylated histones (H3K4me2, H3K9me2, H3K27me2,
191 H3K79me2, H3K4me3, H3K9me3, H3K27me3, and H3K36me3; data not shown).
192

193 **CDX2 enhances cell proliferation in DSS-induced colitis**

194 CDX2 expression is restricted to the nucleus of colon epithelial cells, with decreasing
195 expression in the distal part of the rectum. In the distal part of the colon, CDX2 is expressed only
196 in the superficial cells of the crypts but deviates toward the crypt base in inflammatory states (Fig.
197 4a). The number of CDX2-positive cells was significantly higher in the DSS group (99 ± 2)
198 compared to the control group, but reduced in the DSS+E_2 (51 ± 1) and DSS+G1 (47 ± 4) groups.
199 The antagonist group also showed an increase in CDX2 expression (Fig. 4b). To examine the
200 correlation between CDX2 expression and epithelial cell proliferation, double
201 immunofluorescence analyses were performed using proliferative cell nuclear antigen (PCNA). In
202 the control group, CDX2 and PCNA were differentially expressed, but their expression overlapped
203 in areas of inflammation in the DSS and antagonist groups (Fig. 5). Increased expression of CDX2
204 is associated with enhanced cell proliferation in DSS-induced colitis.

205

206 **Altered expression of claudin-2 and occludin in DSS-induced colitis**

207 In colitis, increased intestinal permeability was shown to be correlated with claudin-2
208 expression (Luettig et al. 2015). Therefore, we examined claudin-2 expression in all experimental
209 groups (Fig. 6a). Increased expression of claudin-2 was observed in the DSS group (35006 ± 4922
210 pixels) compared with the control group, but restrained in the DSS+E_2 (15761 ± 1168 pixels) and
211 DSS+G1 (19771 ± 1012 pixels) groups (Fig. 6b).

212 Occludin is ubiquitously expressed in the epithelial cell membrane, localizing
213 predominantly at apical junctions (Fig. 7a). After DSS treatment, the expression of occludin
214 decreased compared to the control group. Occludin expression was disrupted in the DSS (3461 ±
215 628 pixels) and antagonist groups. The abnormal expression of occludin was ameliorated by E_2
216 and G1 administration. The DSS+E_2 and DSS+G1 treatment groups exhibited preserved occludin
217 expression (14607 ± 1220 pixels and 12631 ± 1322 pixels, respectively) (Fig. 7b).

218

219 **Discussion**

220 The main finding of this study was that estrogen treatment suppresses colonic epithelial
221 damage in mice with DSS-induced colitis. Estrogen enhances the expression of membrane GPR30,
222 H3K36me2, and H3K79me3. Moreover, E_2 and G1 administration reduced cell proliferation and
223 CDX2 expression in DSS-treated mice, thereby affecting tight junction protein expression, which
224 regulates intestinal permeability. These results indicate that estrogen functions through GPR30 to
225 regulate epigenetic modifications and protect the intestinal barrier function against colitis in DSS-
226 treated mice.

227 The estrogen nuclear receptor ERα/ERβ signaling ratio is correlated with the severity of
228 colitis in mice, although details regarding the function of GPR30 are unclear (Goodman et al. 2020).
229 The present study revealed abundant expression of GPR30 in the membrane of cells in normal
230 colon but decreased expression in DSS-induced colitis. The reduction of GPR30 membrane
231 expression in DSS-treated mice was followed by increased GPR30 nuclear expression.
232 The translocation of GPR30 was revealed by decreasing membrane expression and increasing
233 nuclear expression in DSS-induced colitis compared with the normal colon. Nuclear GPR30
234 expression is associated with poor survival outcomes in breast and ovarian carcinomas (Samartzis
235 et al. 2014; Zhu et al. 2018). GPR30 is involved in activation of the PI3K and MAPK/ERK
236 pathways, which results in the expression of transcription factors for numerous genes (Prossnitz
237 and Maggiolini 2009). This result suggests that a correlation exists between inflammation and
238 nuclear GPR30 expression. Treatment with E_2 or G1 reduces inflammation by inhibiting nuclear
239 GPR30 translocation. Immunohistochemistry revealed that E_2 or G1 treatment partially preserved
240 GPR30 membrane expression and reduced nuclear expression. G1 was reported to inhibit nuclear
241 estrogen receptor activity-mediated proliferation of human breast cancer cells and suppress the
242 proliferation of ovarian cancer cells (Smith et al. 2016; Wang et al. 2013). However, the

243 biochemical analyses are required to elucidate the membrane and nuclear fraction of GPR30 in
244 DSS-induced colitis.

245 Recent reports have shown that alteration of histone modifications, such as acetylation and
246 methylation, in colonic epithelial cells is crucial for the onset and progression of colitis (Takeshima
247 et al. 2012; Tsaprouni et al. 2011). An epigenetic-targeted approach using the HDAC inhibitor
248 SAHA effectively controlled local inflammation in DSS-induced colitis by suppressing pro-
249 inflammatory cytokines and chemokines and promoting the accumulation of active inflammatory
250 cells (Ali et al. 2018). Our analyses showed attenuated H3K36me2 and H3K79me3 expression in
251 colonic epithelial cells in DSS-treated mice, whereas E_2 and G1 treatment maintained the
252 expression of H3K36me2 and H3K79me3. Decreased H3K36me2 and H3K79me3 expression in
253 colitis might be caused by activation of lysine demethylase 2B (KDM2B) (Kang et al. 2018).
254 Overexpression of KDM2B reduces the expression of H3K36me2 and H3K79me3 and promotes
255 cell proliferation (Kang et al. 2020; Yan et al. 2018). We demonstrated that treatment with E_2 or
256 G1 significantly inhibits the proliferation of colon epithelial cells, an effect that was blocked by
257 treatment with the antagonist G15. Binding of E_2 and G1 to GPR30 could induce cell-cycle arrest
258 and thereby inhibit cell proliferation (Liu et al. 2017; Wei et al. 2014).

259 The increase of intestinal epithelial cells (IEC) proliferation was found to overlap with
260 CDX2 expression in DSS-treated mice. Cell proliferation and CDX2 are differentially expressed
261 in normal epithelial cells. Our study showed that inflammation is associated with increased cell
262 proliferation and CDX2 expression in DSS-induced colitis. CDX2 regulates the expression of
263 ubiquitous genes that play important roles in controlling cell dynamics, including cell proliferation
264 (Saad, 2011). Expression of CDX2 is increased in DSS-induced colitis in mice but inhibited by E_2
265 and G1 administration. Increased CDX2 expression could affect intestinal permeability by altering
266 the expression of tight junction proteins. Previous studies have shown that increased CDX2

expression elicited by IL-6 involves the PI3K and MEK/ERK pathways in IECs, resulting in increased claudin-2 expression (Suzuki et al. 2011). Claudin-2 is predominantly expressed in leaky epithelia and contributes to diarrhea in many intestinal diseases via leak flux mechanisms (Luettig et al. 2015). In the present study, the expression of claudin-2 was increased in DSS-treated mice but inhibited by E_2 and G1 treatment. Moreover, occludin expression in the epithelial cell membrane was decreased in DSS-induced colitis but maintained by E_2 and G1 treatment. G1 is also reported to reduce tight junction disorders through the expression of VEGF-A after ischemia injury (Lu et al. 2016). The intestinal barrier defects in colitis associated with increased claudin-2 expression accompanied by the downregulated expression of barrier-forming tight junction proteins such as occludin (Luettig et al. 2015). Based on our results, we suggest that estrogen functions through GPR30 to protect intestinal permeability by alleviating claudin-2 overexpression and maintaining occludin expression in DSS-induced colitis in mice.

In conclusion, the present study demonstrated that estrogen functions through GPR30 to affect histone modifications that control cell proliferation and regulates CDX2 expression, which protects the intestinal epithelial barrier function in mice with DSS-induced colitis. This finding suggests that GPR30 plays a crucial role in maintaining intestinal epithelial homeostasis and may be an important target for colitis therapies. Further studies are required to elucidate the molecular mechanism of GPR30 in IBD.

Acknowledgments

This study was partly supported by a Grant-in-Aid for Scientific Research from the Japan Society for the Promotion of Science (No. 16K08471, No. 21K06738 to Y. Hishikawa).

Conflict of interest: We have *no conflict of interest* to declare.

Data availability

The corresponding author will provide original micrographs and further information upon reasonable request.

296 **References**

297 Ali MN, Choijookhuu N, Takagi H, Srisowanna N, Huynh MNN, Yamaguchi Y, Oo PS, Kyaw
298 MTH, Sato K, Yamaguchi R., Hishikawa Y (2018) The HDAC inhibitor, SAHA, prevents
299 colonic inflammation by suppressing pro-inflammatory cytokines and chemokines in DSS-
300 induced colitis. Acta Histochem Cytochem 51(1):33–40. https://doi.org/10.1267/ahc.17033
301 Bábíčková J, Tóthová Ľ, Lengyelová E, Bartoňová A, Hodosy J, Gardlík R, Celec P (2015) Sex
302 differences in experimentally induced colitis in mice: a role for estrogens. Inflammation
303 38(5);1996–2006. https://doi.org/10.1007/s10753-015-0180-7
304 Chelakkot C, Ghim J, Ryu SH (2018) Mechanisms regulating intestinal barrier integrity and its
305 pathological implications. Exp Mol Med 50(103):1-9. Nature Publishing Group.
306 https://doi.org/10.1038/s12276-018-0126-x
307 Choijookhuu N, Shibata Y, Ishizuka T, Xu Y, Koji T, Hishikawa Y (2022) An Advanced Detection
308 System for In Situ Hybridization Using a Fluorescence Resonance Energy Transfer-based
309 Molecular Beacon Probe. Acta Histochem Cytochem 55(5):119–128.
310 https://doi.org/10.1267/ahc.22-00075
311 Cooper HS, Murthy SN, Shah RS, Sedergran, DJ (1993) Clinicopathologic study of dextran sulfate
312 sodium experimental murine colitis. Lab Invest 69:238–249
313 Dalal SR, Chang EB (2014) The microbial basis of inflammatory bowel diseases. J Clin Invest
314 124(10):4190–4196. https://doi.org/10.1172/JCI72330
315 De Francesco EM, Pellegrino M, Santolla MF, Lappano R, Ricchio E, Abonante S, Maggiolini M
316 (2014) GPER mediates activation of HIF1α/VEGF signaling by estrogens. Cancer Res
317 74(15):4053–4064. https://doi.org/10.1158/0008-5472.CAN-13-3590
318 Forss A, Clements M, Bergman D, Roelstraete B, Kaplan GG, Myrelid P, Halfvarson J, Olén O,
319 Ludvigsson JF (2022) A nationwide cohort study of the incidence of inflammatory bowel

320 disease in Sweden from 1990 to 2014. Aliment Pharmacol Ther 55(6):691–699.
321 https://doi.org/10.1111/apt.16735
322 Gonçalves C, Schneider N, Mello HF, Passos EP (2013) Characterization of acute murine dextran
323 sodium sulfate (DSS) colitis: severity of inflammation is dependent on the DSS molecular
324 weight and concentration. Acta Sci Vet 41(1):1–9
325 Goodman WA, Bedoyan SM, Havran HL, Richardson B, Cameron MJ, Pizarro TT (2020) Impaired
326 estrogen signaling underlies regulatory T cell loss-of-function in the chronically inflamed
327 intestine. Proc Natl Acad Sci USA 117(29):17166–17176
328 https://doi.org/10.1073/pnas.2002266117/-/DCSupplemental
329 Goodman WA, Havran HL, Quereshy HA, Kuang S, De Salvo C, & Pizarro TT (2018) Estrogen
330 receptor α loss-of-function protects female mice from DSS-induced experimental colitis. Cell
331 Mol Gastroenterol Hepatol 5(4):630-633.e1. https://doi.org/10.1016/j.jcmgh.2017.12.003
332 Heller F, Fromm A, Gitter AH, Mankertz J, Schulzke JD (2008) Epithelial apoptosis is a prominent
333 feature of the epithelial barrier disturbance in intestinal inflammation: effect of pro-
334 inflammatory interleukin-13 on epithelial cell function. Mucosal Immunol 1:58–61.
335 https://doi.org/10.1038/mi.2008.46
336 Jacenik D, Zielińska M, Mokrowiecka A, Michlewska S, Małecka-Panas E, Kordek R, Fichna J,
337 Krajewska WM (2019) G protein-coupled estrogen receptor mediates anti-inflammatory
338 action in crohn's disease. Sci Rep 9(1):1–13. https://doi.org/10.1038/s41598-019-43233-3
339 Kaimaktchiev V, Terracciano L, Tornillo L, Spichtin H, Stoios D, Bundi M, Korcheva V, Mirlacher,
340 M, Loda M, Sauter G, Corless CL (2004) The homeobox intestinal differentiation factor
341 CDX2 is selectively expressed in gastrointestinal adenocarcinomas. Mod Pathol 17(11):
342 1392–1399. https://doi.org/10.1038/modpathol.3800205

343 Kang JY, Kim JY, Kim KB, Park JW, Cho H, Hahm JY, Chae YC, Kim D, Kook H, Rhee S, Ha
344 NC, Seo SB (2018) KDM2B is a histone H3K79 demethylase and induces transcriptional
345 repression via sirtuin-1–mediated chromatin silencing. FASEB J 32(10):5737–5750.
346 https://doi.org/10.1096/fj.201800242R
347 Kang JY, Park JW, Hahm JY, Jung H, Seo, SB (2020) Histone H3K79 demethylation by KDM2B
348 facilitates proper DNA replication through PCNA dissociation from chromatin. Cell Prolif
349 53(11). https://doi.org/10.1111/cpr.12920
350 Liu Q, Chen Z, Jiang G, Zhou Y, Yang X, Huang H, Liu H, Du, J, Wang H (2017) Epigenetic down
351 regulation of G protein-coupled estrogen receptor (GPER) functions as a tumor suppressor
352 in colorectal cancer. Mol. Cancer 16(1):1–14. https://doi.org/10.1186/s12943-017-0654-3
353 Lu D, Qu Y, Shi F, Feng D, Tao K, Gao G, He S, Zhao T (2016) Activation of G protein-coupled
354 estrogen receptor 1 (GPER-1) ameliorates blood-brain barrier permeability after global
355 cerebral ischemia in ovariectomized rats. Biochem. Biophys. Res. Commun.. 477(2):209–
356 214. https://doi.org/10.1016/j.bbrc.2016.06.044
357 Luettig J, Rosenthal R, Barmeyer C, Schulzke JD (2015) Claudin-2 as a mediator of leaky gut
358 barrier during intestinal inflammation. Tissue Barriers 3(1):1–2.
359 https://doi.org/10.4161/21688370.2014.977176
360 Mankertz, J, Amasheh M, Krug SM, Fromm A, Amasheh S, Hillenbrand B, Tavalali S, Fromm M,
361 Schulzke JD (2009) TNFα up-regulates claudin-2 expression in epithelial HT-29/B6 cells via
362 phosphatidylinositol-3-kinase signaling. Cell Tissue Res 336(1):67–77.
363 https://doi.org/10.1007/s00441-009-0751-8
364 Mateos B, Palanca-Ballester C, Saez-Gonzalez E, Moret I, Lopez A, Sandoval J (2019) Epigenetics
365 of inflammatory bowel disease: unraveling pathogenic events. Crohn's and Colitis 360
366 1(2):1-4. https://doi.org/10.1093/crocol/otz017

367 Prossnitz ER, Maggiolini M (2009) Mechanisms of estrogen signaling and gene expression via
368 GPR30. Mol Cell 308(1–2):32–38. https://doi.org/10.1016/j.mce.2009.03.026
369 Saad RS (2011) CDX2 as a marker for intestinal differentiation: its utility and limitations. World
370 J. Gastrointest Surg 3(11):159. https://doi.org/10.4240/wjgs.v3.i11.159
371 Samartzis EP, Noske A, Meisel A, Varga Z, Fink D, Imesch P (2014) The G protein-coupled
372 estrogen receptor (GPER) is expressed in two different subcellular localizations reflecting
373 distinct tumor properties in breast cancer. PLoS One.
374 https://doi.org/10.1371/journal.pone.0083296
375 Shirouzu S, Sugita N, Choijookhuu N, Yamaguma Y, Takeguchi K, Ishizuka T, Tanaka M, Fidya,
376 Kai K, Chosa E, Yamashita Y, Koshimoto C, Hishikawa Y (2022) Pivotal role of high-
377 mobility group box 2 in ovarian folliculogenesis and fertility. J Ovarian Res, 15(133):1-11.
378 https://doi.org/10.1186/s13048-022-01071-4
379 Shivashankar R, Tremaine, WJ, Harmsen, WS, Loftus EV (2017) Incidence and Prevalence of
380 Crohn's Disease and Ulcerative Colitis in Olmsted County, Minnesota From 1970 Through
381 2010. Clin. Gastroenterol. Hepatol. *5*(6), 857–863. https://doi.org/10.1016/j.cgh.2016.10.039
382 Smith LC, Ralston-Hooper KJ, Ferguson LL, Sabo-Attwood T (2016) The G protein-coupled
383 estrogen receptor agonist G-1 inhibits nuclear estrogen receptor activity and stimulates novel
384 phosphoproteomic signatures. Toxicol. Sci., 151(2):434–446.
385 https://doi.org/10.1093/toxsci/kfw057
386 Suzuki, T, Yoshinaga N, Tanabe S. (2011). Interleukin-6 (IL-6) regulates claudin-2 expression and
387 tight junction permeability in intestinal epithelium. *Journal of Biological Chemistry*, *286*(36),
388 31263–31271. https://doi.org/10.1074/jbc.M111.238147

389 Takeshima H, Ikegami D, Wakabayashi M, Niwa T, Kim YJ, Ushijima T (2012) Induction of
390 aberrant trimethylation of histone H3 lysine 27 by inflammation in mouse colonic epithelial
391 cells. Carcinogenesis 33(12):2384–2390. https://doi.org/10.1093/carcin/bgs294
392 Tan Y, Guan Y, Sun Y, Zheng C (2019) Correlation of intestinal mucosal healing and tight junction
393 protein expression in ulcerative colitis patients. Am J Med Sci 357(3):195–204.
394 https://doi.org/10.1016/j.amjms.2018.11.011
395 Tsaprouni LG, Ito K, Powell JJ, Adcock IM, Punchard N (2011) Differential patterns of histone
396 acetylation in inflammatory bowel diseases. J. Inflamm 8(1):1-12.
397 https://doi.org/10.1186/1476-9255-8-1
398 Verdú EF, Verdú V, Deng Y, Bercik P, Collins SM (2002) Modulatory effects of estrogen in two
399 murine models of experimental colitis. Am J Physiol Gastrointest Liver Physiol 283(1):G27-
400 36. https://doi.org/10.1152/ajpgi.00460.2001.
401 Wang C, Lv X, He C, Hua G, Tsai MY, Davis JS (2013) The G-protein-coupled estrogen receptor
402 agonist G-1 suppresses proliferation of ovarian cancer cells by blocking tubulin
403 polymerization. Cell Death and Dis 4(10). https://doi.org/10.1038/cddis.2013.397
404 Wei W, Chen ZJ, Zhang KS, Yang XL, Wu YM, Chen XH, Huang HB, Liu HL, Cai SH, Du J,
405 Wang HS (2014) The activation of G protein-coupled receptor 30 (GPR30) inhibits
406 proliferation of estrogen receptor negative breast cancer cells in vitro and in vivo. Cell Death
407 5(1):e1428. https://doi.org/10.1038/cddis.2014.398
408 Yamaguma Y, Sugita N, Choijookhuu N, Yano K, Lee D, Ikenoue M, Fidya, Shirouzu S, Ishizuka
409 T, Tanaka M, Yamashita Y, Chosa E, Taniguchi N, Hishikawa Y (2022) Crucial role of high-
410 mobility group box 2 in mouse ovarian follicular development through estrogen receptor beta.
411 Histochem Cell Biol 157(3), 359–369. https://doi.org/10.1007/s00418-022-02074-4

412 Yan M, Yang X, Wang H, Shao Q (2018) The critical role of histone lysine demethylase KDM2B
413 in cancer. Am J Transl Res 10(8):2222–2233.
414 Yano K, Choijookhuu N, Ikenoue M, Fidya, Fukaya T, Sato K, Lee D, Taniguchi N, Chosa, E,
415 Nanashima A, Hishikawa Y (2022) Spatiotemporal expression of HMGB2 regulates cell
416 proliferation and hepatocyte size during liver regeneration. Sci Rep 12(1):1–13.
417 https://doi.org/10.1038/s41598-022-16258-4
418 Zhu CX, Xiong W, Wang ML, Yang J, Shi HJ, Chen HQ, Niu G (2018) Nuclear G protein-coupled
419 oestrogen receptor (GPR30) predicts poor survival in patients with ovarian cancer. J Int Med
420 46(2):723–731. https://doi.org/10.1177/0300060517717625
421 Zielińska M, Fichna J, Bashashati M, Habibi S, Sibaev A, Timmermans JP, Storr M (2017) G
422 protein-coupled estrogen receptor and estrogen receptor ligands regulate colonic motility and
423 visceral pain. Neurogastroenterol Motil 29(7) :1-11. https://doi.org/10.1111/nmo.13025
424

425 **Figure legends**

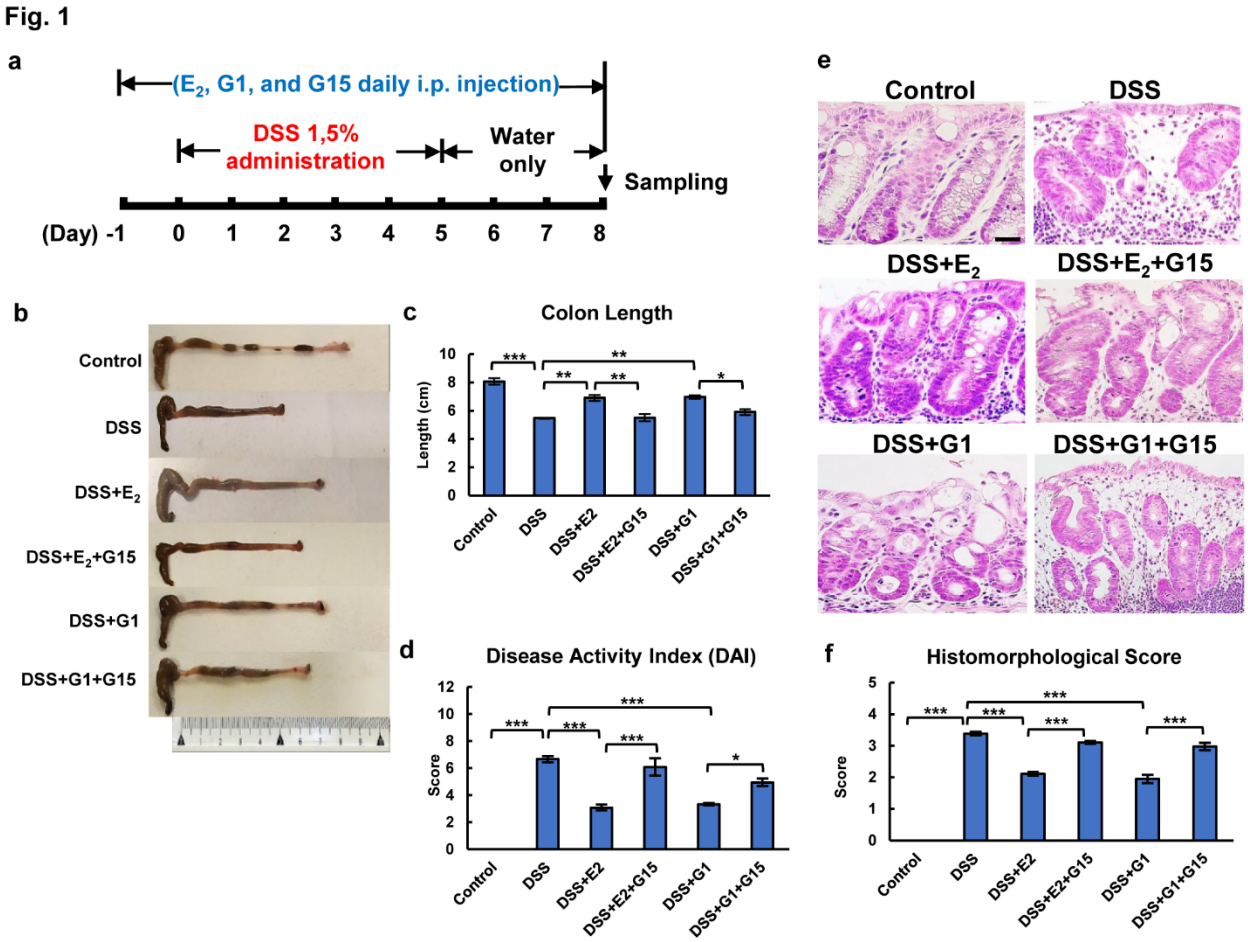

426

427 **Fig. 1 E_2 and G1 protect from intestinal tissue damage in DSS-induced colitis.**

428 **a** Schematic diagram of DSS-induced colitis mice treated with 17β-estradiol (E_2), agonist-GPR30

429 (G1), or antagonist-GPR30 (G15). **b** Macroscopic changes in colon tissue of control, DSS-,

430 DSS+E_2–, DSS+E_2+G15–, DSS+G1–, and DSS+G1+G15–treated mice, colon length (**c**), and DAI

431 (**d**). **e** HE staining and histomorphological evaluation (**f**) of colon tissues of all experimental mice.

432 Data shown in the graphs are presented as the mean ± SEM. In each experimental group, three mice

433 were used. Scale bar: 20 μm; magnification 400×. * $p<0.05$, ** $p<0.01$, ***$p<0.001$.

434

435

Fig. 2

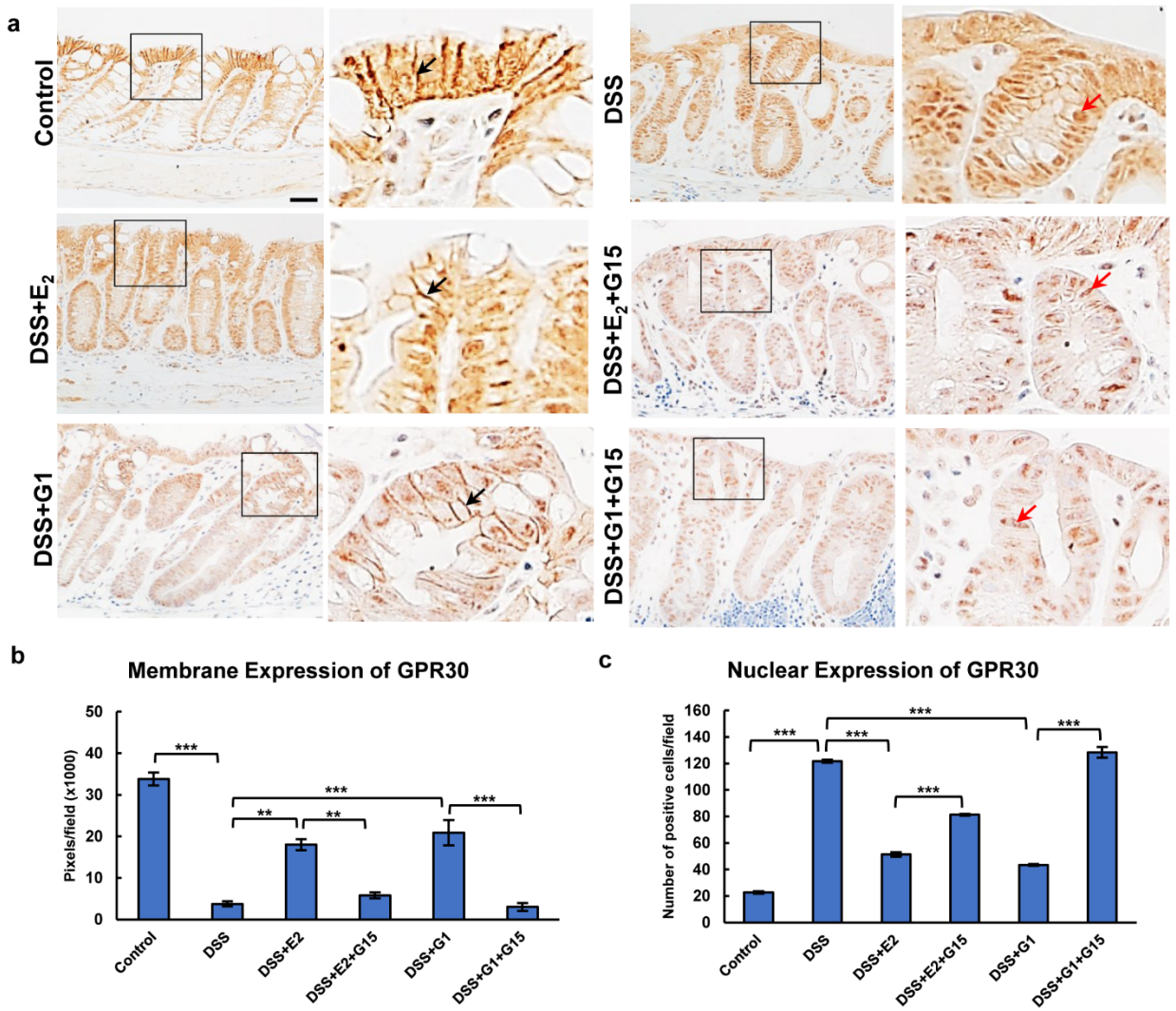

Fig. 2 Subcellular localization of GPR30 in DSS-induced colitis.

a Immunohistochemical expression of GPR30 in colon tissue of control, DSS-, DSS+E_2–, DSS+E_2+G15–, DSS+G1–, and DSS+G1+G15–treated mice. Insets are magnified on right side. Black arrows indicate positive membrane expression. Red arrows indicate positive nuclear expression. **b** GPR30 epithelial cell expression in the membrane (pixels/field ×1,000) and nucleus (**c**). Data in the graphs are presented as the mean ± SEM. In each experimental group, three mice were used. Scale bar: 20 µm; magnification 400×. ** $p<0.01$, *** $p<0.001$.

Fig. 3

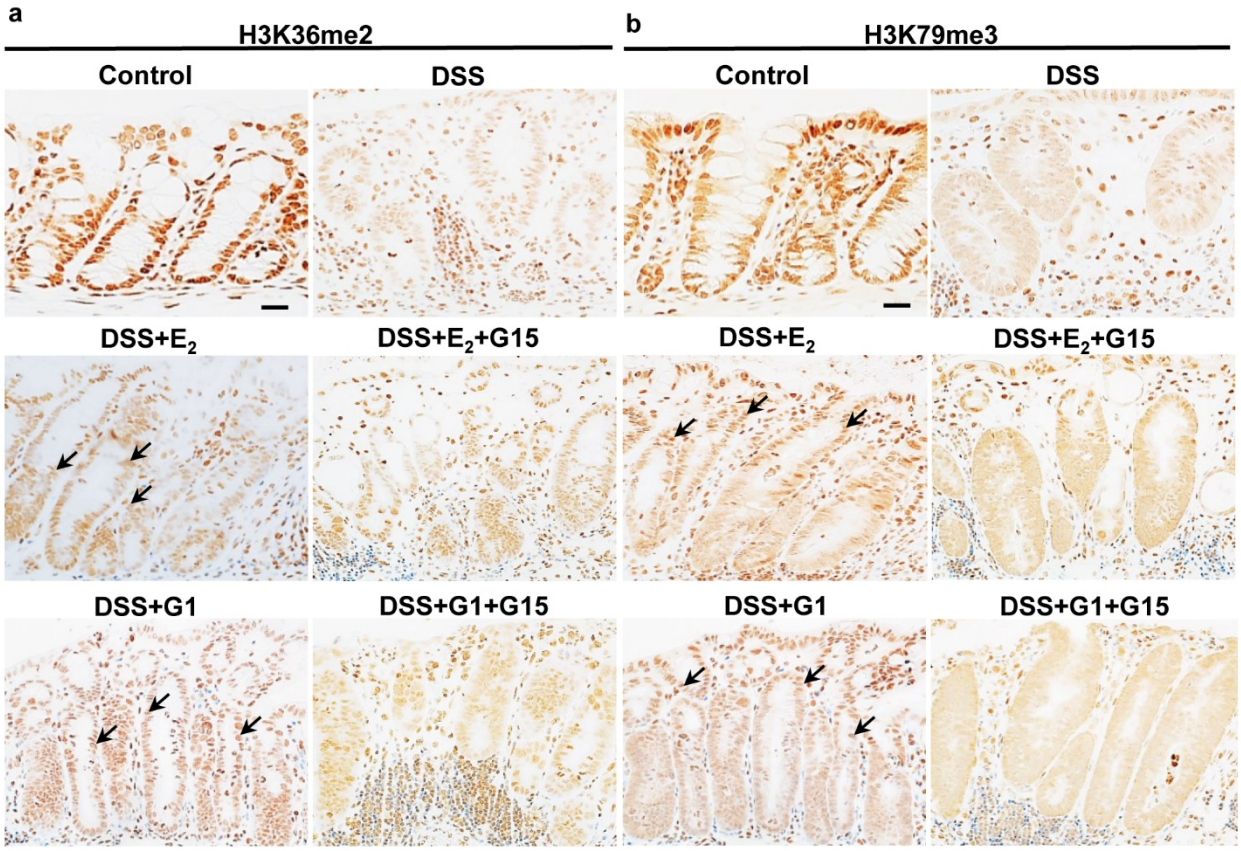

445

446 **Fig. 3 Expression of H3K36me2 and H3K79me3 in DSS-induced colitis.**

447 **a** Immunohistochemical localization of H3K36me2 and H3K79me3 (**b**) in the colon of control,
448 DSS-, DSS+E_2–, DSS+E_2+G15–, DSS+G1–, and DSS+G1+G15–treated mice. Black arrows
449 indicate H3K36me2- and H3K79me3-positive epithelial cells. Scale bar: 20 μm; magnification
450 400×.

Fig. 4

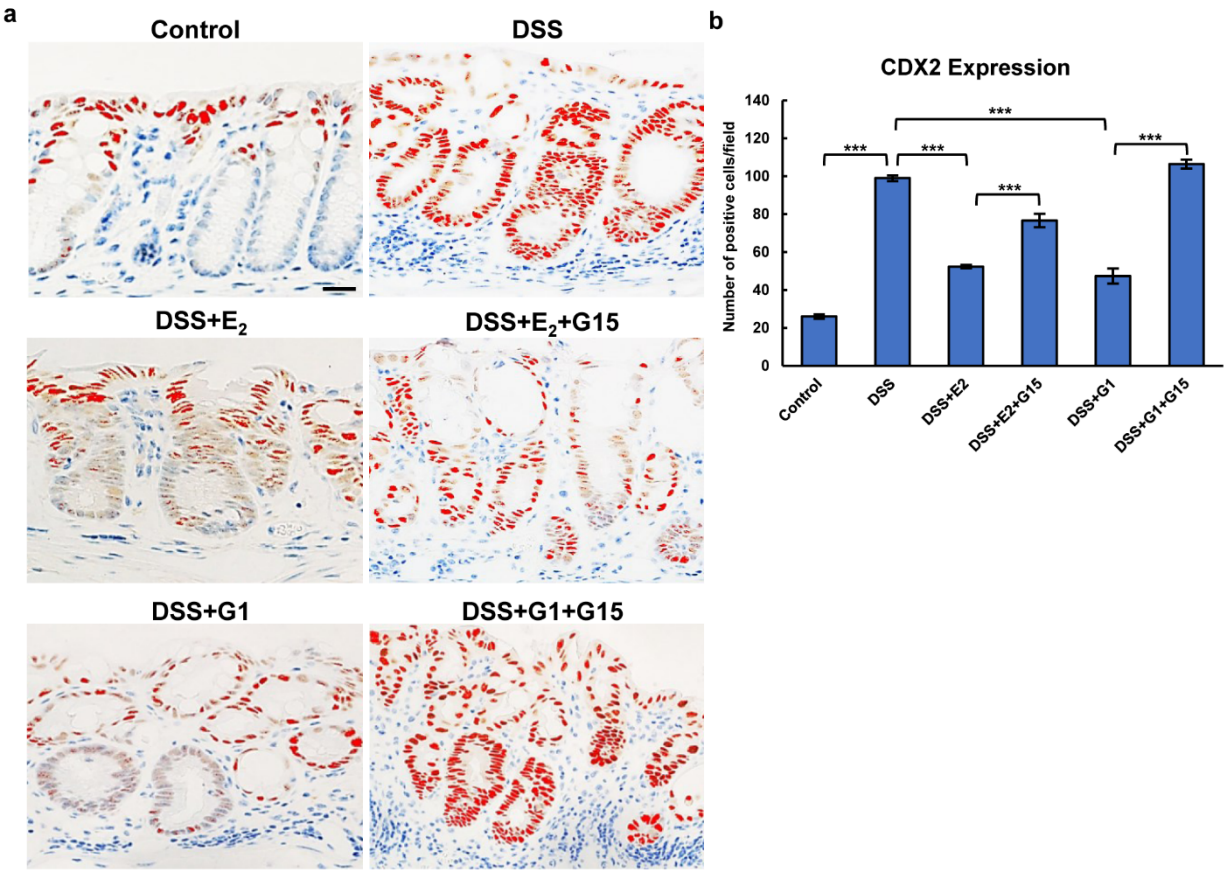

451

452 **Fig. 4 Immunohistochemical localization of CDX2 in DSS-induced colitis.**

453 Immunohistochemical analysis of the expression of CDX2 in DSS-induced colitis. **a** CDX2

454 localization in colon tissue of control, DSS-, DSS+E_2–, DSS+E_2+G15–, DSS+G1–, and

455 DSS+G1+G15–treated mice. Red color represents positive cells according to WinROOF image

456 analysis. **b** Number of CDX2-positive cells. Data in the graphs are presented as the mean ± SEM.

457 In each experimental group, three mice were used. Scale bar: 20 μm; magnification 400×. **

458 $p<0.01$, *** $p<0.001$.

459

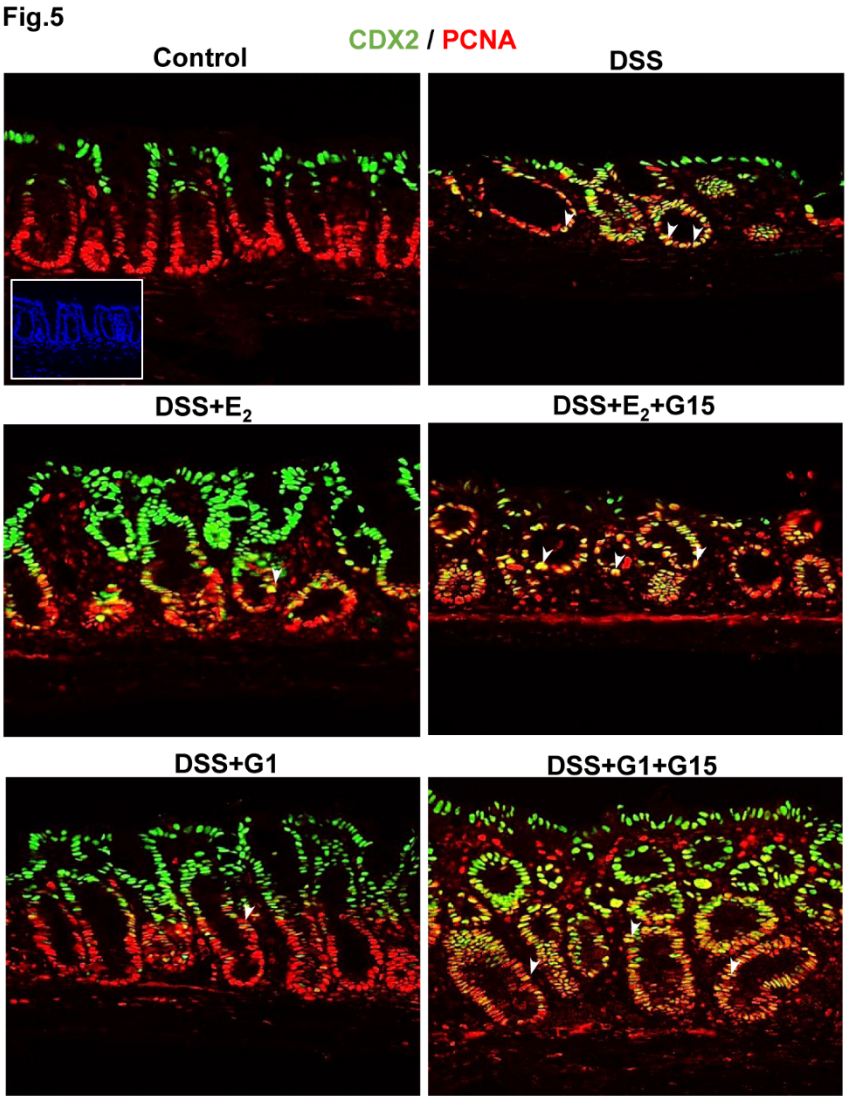

460

461 **Fig. 5 Co-localization of CDX2 and PCNA in colonic epithelial cells.**

462 Double immunofluorescence analysis of CDX2 (green) and PCNA (red) in DSS-induced colitis.

463 High-magnification microphotographs are shown. White arrows indicate double-positive cells.

464 Cell nuclei were counterstained with DAPI in every experiment. Scale bar: 50 μm; magnification

465 400×.

Fig. 6

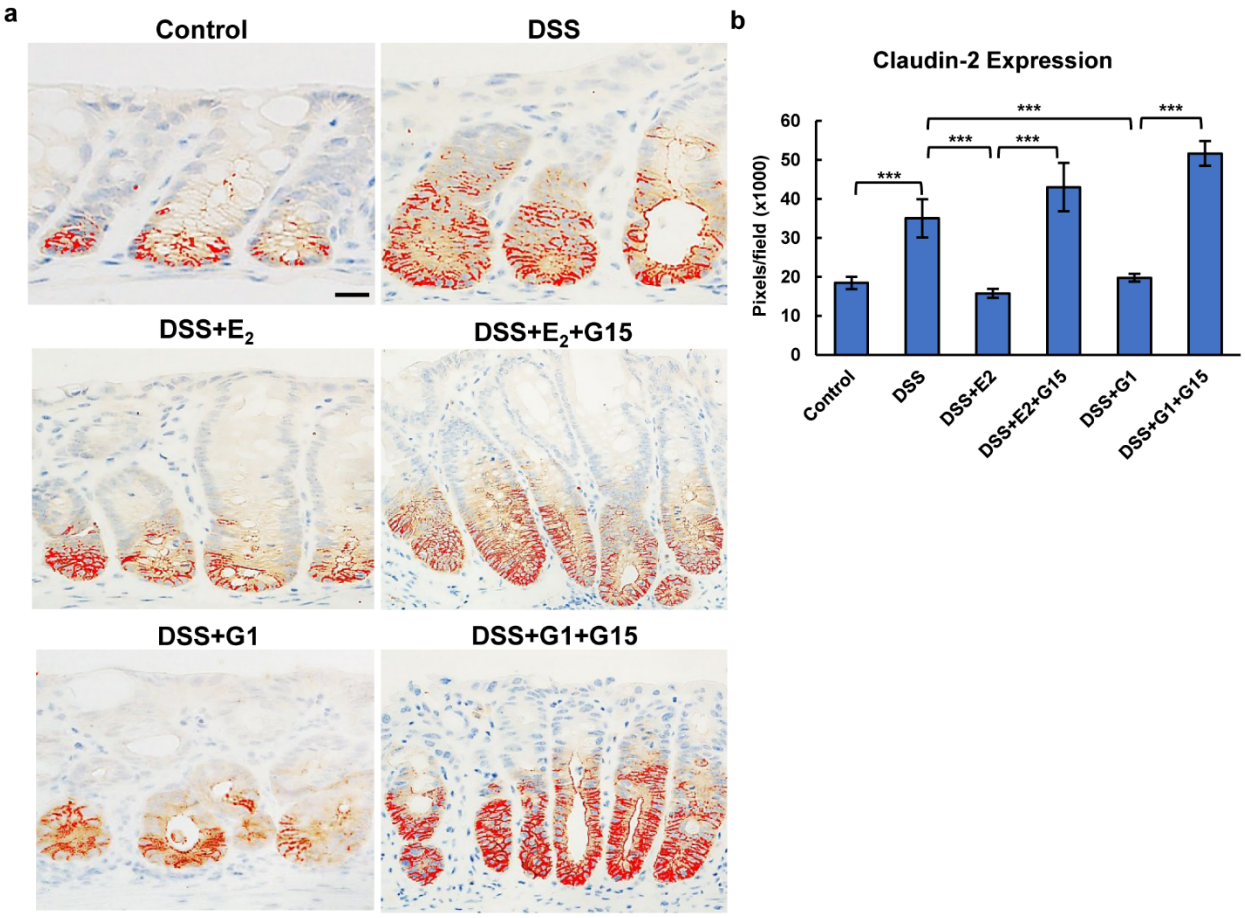

466

467 **Fig. 6 Localization of claudin-2 in DSS-induced colitis.**

468 **a** Immunohistochemical analysis of the expression of claudin-2 in the colon of control, DSS-,
469 DSS+E_2–, DSS+E_2+G15–, DSS+G1–, and DSS+G1+G15–treated mice. **b** Claudin-2 epithelial cell
470 expression in the membrane (pixels/field ×1,000). Red color represents a positive membrane
471 according to WinROOF image analysis. Data in the graphs are presented as the mean ± SEM. In
472 each experimental group, three mice were used. Scale bar: 20 μm; magnification 400×. *p <0.05,
473 ** p<0.01.

Fig. 7

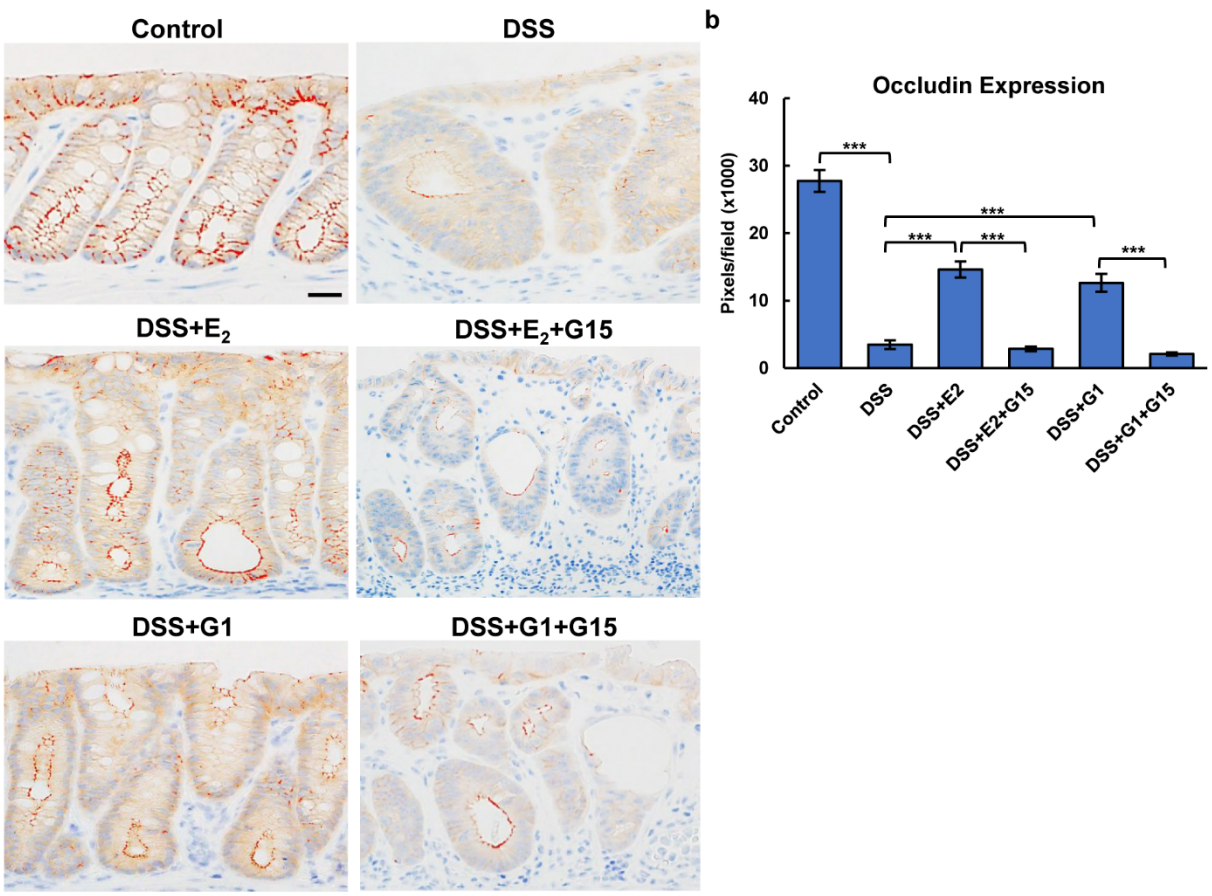

Fig. 7 Localization of occludin in DSS-induced colitis mice.

a Immunohistochemical analysis of the expression of occludin in the colon of control, DSS-, DSS+E_2–, DSS+E_2+G15–, DSS+G1–, and DSS+G1+G15–treated mice. **b** Occludin epithelial cell expression in the membrane (pixels/field ×1,000). Red color represents a positive membrane according to WinROOF image analysis. Data in the graphs are presented as the mean ± SEM. In each experimental group, three mice were used. Scale bar: 20 μm; magnification 400×. ** $p<0.01$, *** $p<0.001$.

Fig. 8

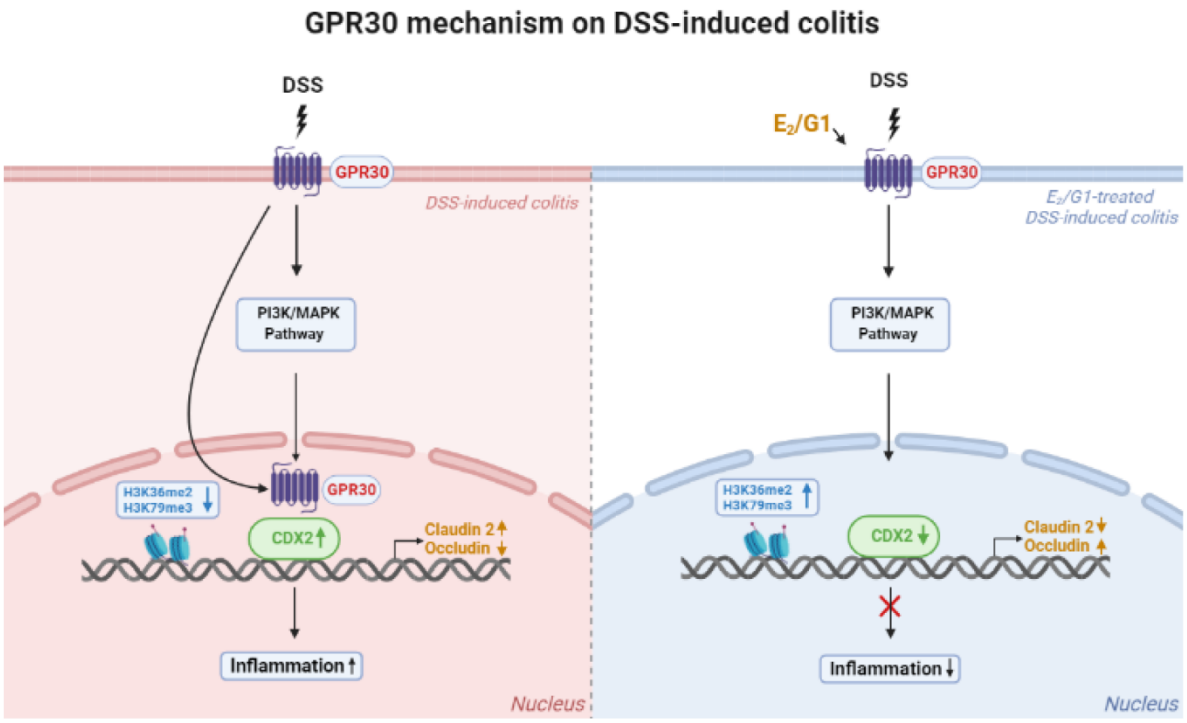

Fig. 8 Schematic diagram of GPR30 mechanism on DSS-induced colitis. E_2 and G1 inhibit GPR30 nuclear translocation by involving PI3K/MAPK pathway, which increases H3K36me2 and H3K79me3 and suppresses CDX2 expressions. Decreased CDX2 reduces claudin2 and increases occludin expressions. (Created with BioRender.com)